

# Coulomb charging energy for arbitrary tunneling strength

Xiaohui Wang, Reinhold Egger, and Hermann Grabert

*Fakultät für Physik, Albert-Ludwigs-Universität Freiburg, Hermann-Herder-Straße 3, D-79104 Freiburg*

The Coulomb energy of a small metallic island coupled to an electrode by a tunnel junction is investigated. We employ Monte Carlo simulations to determine the effective charging energy for arbitrary tunneling strength. For small tunneling conductance, the data agree with analytical results based on a perturbative treatment of electron tunneling, while for very strong tunneling recent semiclassical results for large conductance are approached. The data allow for an identification of the range of validity of various analytical predictions.

PACS numbers: 73.40.Gk, 73.40.Rw, 74.50.+r

Charging effects in metallic nanostructures [1] continue to be studied extensively both theoretically and experimentally. While for the case of weak tunneling the underlying physics is well understood [2] and starts to find metrological applications [3], for the case of strong tunneling there are several conflicting analytical predictions [4–14]. To settle these discrepancies, we have performed precise Monte Carlo calculations for a large range of the tunneling strength.

The simplest device displaying Coulomb charging effects is the single electron box (SEB) which is formed by a metallic island between a tunnel junction and a gate capacitor, see Fig. 1. The external electrodes are biased by a voltage source. If the tunneling resistance  $R_t$  is large compared to  $R_K = h/e^2 \sim 25.8 \text{ k}\Omega$ , the charge  $q$  on the metallic island is quantized,  $q = -ne$ , where  $n$  is the number of excess electrons on the island. A simple electrostatic calculation for vanishing electron tunneling gives for the ground state an electron number  $n$  which is the integer closest to  $n_{\text{ex}} = C_g U/e$ . Hence, as a function of the applied voltage,  $n$  displays the well-known Coulomb staircase.

At finite temperature the Coulomb staircase is rounded by thermal fluctuations of the island charge. This thermal smearing is easily understood and seen experimentally [15]. However, there is also a quantum-mechanical rounding of the steps, since the island charge is not truly quantized. Electron tunneling leads to hybridization of the states in the lead and island electrodes. For very strong tunneling, we expect a complete washout of charging effects, and the average electron number  $\langle n \rangle$  in the box becomes proportional to the applied voltage,  $\langle n \rangle = n_{\text{ex}}$ . As indicated in Fig. 1, there is a gradual breakdown of the Coulomb blockade behavior as the dimensionless tunneling conductance  $\alpha_t = R_K/R_t$  increases.

The classical single electron charging energy of the SEB is given by  $E_c = e^2/2C$ , where the island capacitance  $C$  is the sum of the capacitance  $C_t$  of the tunnel junction and the gate capacitance  $C_g$  (see Fig. 1). This quantity can be extracted from measurements in

the classical regime [15]. The strength of the Coulomb blockade effect may be described in terms of an effective charging energy  $E_c^*$  which coincides with  $E_c$  in the limit of small quantum fluctuations of the charge,  $\alpha_t \ll 1$ , and vanishes in the limit of strong tunneling,  $\alpha_t \gg 1$ . Since in the latter case  $\partial \langle n \rangle / \partial n_{\text{ex}} \rightarrow 1$ , we may define  $E_c^*$  from the slope of the staircase at  $n_{\text{ex}} = 0$  by

$$E_c^* = E_c (1 - \partial \langle n \rangle / \partial n_{\text{ex}}|_{n_{\text{ex}}=0}) .$$

A completely equivalent definition of  $E_c^*$  in terms of the free energy  $F(n_{\text{ex}}, \alpha_t)$  of the SEB reads

$$E_c^* = \frac{1}{2} \frac{\partial^2 F(n_{\text{ex}}, \alpha_t)}{\partial n_{\text{ex}}^2} \Big|_{n_{\text{ex}}=0} . \quad (1)$$

Several previous articles have made analytical predictions on  $E_c^*/E_c$  as a function of  $\alpha_t$ . For small  $\alpha_t$ , perturbation theory in the tunneling term may be employed. One finds at zero temperature [16]

$$E_c^*/E_c = 1 - (1/\pi^2)\alpha_t + d_2\alpha_t^2 + \mathcal{O}(\alpha_t^3) .$$

The linear term is readily evaluated [5]. For higher-order corrections one must take into account that the charging energy in the unperturbed Hamiltonian leads to a correlation of the Fermi liquids in the lead and island electrodes. Based on the non-crossing approximation (NCA), Golubev and Zaikin [9] find (see Eq. (8) in Ref. [9])

$$d_2 = \frac{1}{8\pi^4} \left( \frac{7\pi^2 - 64}{12} + \frac{29 \ln(2)}{9} - 4 \ln(2) \ln(3) + 2 \text{Li}_2(3/4) \right) = 3.134/16\pi^4 , \quad (2)$$

where  $\text{Li}_2(x) = -\int_0^x dz \ln(1-z)/z$  is the dilogarithm function. On the other hand, from the systematic evaluation of all diagrams, Grabert [8,10] obtains (see Eq. (2) in Ref. [8] or Eq. (100) in Ref. [10])

$$d_2 = \frac{1}{8\pi^4} \left( \frac{4\pi^2 - 16}{3} + \frac{32 \ln(2)}{9} - 8 \ln^2(2) - 4 \text{Li}_2(3/4) \right) = 5.066/16\pi^4 . \quad (3)$$

The difference between Eqs. (2) and (3) indicates that the NCA becomes a poor approximation for large  $\alpha_t$ .

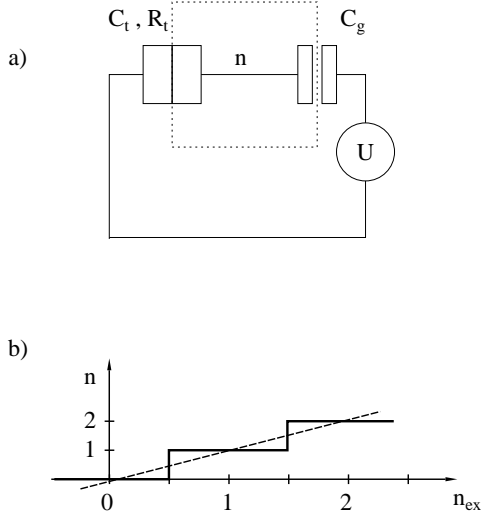


FIG. 1. a) The circuit diagram of the single-electron box, consisting of a tunnel junction in series with a capacitor  $C_g$ . The junction resistance is  $R_t$  and the junction capacitance is  $C_t$ . b) The number  $n$  of electrons in the box as a function of the applied voltage  $U = (e/C_g)n_{\text{ex}}$  in the Coulomb blockade regime,  $R_t \gg R_K$  (solid line) and for strong tunneling,  $R_t \ll R_K$  (dashed line).

The case of strong tunneling,  $\alpha_t \gg 1$ , was first studied by Panyukov and Zaikin [6]. Based on an instanton approach [17], these authors find (see Eqs. (7) and (8) in Ref. [6])

$$E_c^*/E_c = \alpha_t^2 \exp(-\alpha_t/2 + \gamma), \quad (4)$$

where  $\gamma = 0.577\dots$  is Euler's constant. Very recently, Wang and Grabert have evaluated the low-temperature partition function of the SEB by related path-integral methods [14]. For large  $\alpha_t$ , the path integral is dominated by multi-sluggon trajectories whose contribution can be summed analytically yielding (Eq. (10) in Ref. [14])

$$E_c^*/E_c = 2\alpha_t^3 e^{-\alpha_t/2} [1 + \mathcal{O}(\ln(\alpha_t)/\alpha_t)]. \quad (5)$$

The exponential dependence of  $E_c^*$  on  $\alpha_t$  in Eqs. (4) and (5) is in accordance with a recent renormalization-group analysis [12]. However, the pre-exponential factors differ by orders of magnitude in the strong-tunneling regime. Available renormalization-group techniques do not resolve this problem.

To clarify the discrepancies and identify reliable methods for further analytical work, we have performed Monte Carlo (MC) simulations. We start from the path integral

for the partition function of the SEB which may be written as

$$Z(n_{\text{ex}}, \alpha_t) = \int D[\varphi] e^{-S_{\text{box}}[\varphi]}, \quad (6)$$

where  $\beta = 1/k_B T$  is the inverse temperature, and the integral is over all paths of the phase  $\varphi(\tau)$  in the interval  $-\beta/2 \leq \tau \leq \beta/2$  with  $\varphi(\beta/2) = \varphi(-\beta/2)$  modulus  $2\pi$ . The action

$$S_{\text{box}}[\varphi] = S_c[\varphi] + S_t[\varphi]$$

contains two parts describing charging of the island and tunneling across the junction. The effect of the Coulomb energy is contained in

$$S_c[\varphi] = \int_{-\beta/2}^{\beta/2} d\tau \left[ \frac{1}{4E_c} (\dot{\varphi} + 2in_{\text{ex}}E_c)^2 + E_c n_{\text{ex}}^2 \right].$$

The second part of the action [18]

$$S_t[\varphi] = 2 \int_{-\beta/2}^{\beta/2} d\tau \int_{-\beta/2}^{\beta/2} d\tau' \alpha(\tau - \tau') \sin^2 \left[ \frac{\varphi(\tau) - \varphi(\tau')}{2} \right]$$

describes tunneling. The Fourier transform of  $\alpha(\tau)$  reads  $\alpha_l = -\alpha_t |\omega_l|/4\pi$  for  $|\omega_l| \ll D$ , where  $\omega_l = 2\pi l/\beta$  are the Matsubara frequencies and  $D$  is the electronic bandwidth.

By using the definition (1) for the effective charging energy, we can relate  $E_c^*$  to the partition function,

$$E_c^* = -\frac{1}{2\beta} \frac{\partial^2 \ln Z(n_{\text{ex}}, \alpha_t)}{\partial n_{\text{ex}}^2} \Big|_{n_{\text{ex}}=0}. \quad (7)$$

To proceed, we write Eq. (6) in the equivalent form

$$Z(n_{\text{ex}}, \alpha_t) = \sum_{m=-\infty}^{\infty} e^{2\pi i m n_{\text{ex}}} \int D[\vartheta] \exp(-S_m[\vartheta]), \quad (8)$$

where we have separated the functional integration into a sum over winding numbers  $m$  and an integration over all paths  $\vartheta(\tau)$  which are now subject to the boundary conditions  $\vartheta(-\beta/2) = \vartheta(\beta/2) = 0$ . Here, the action  $S_m[\vartheta]$  is given by

$$S_m[\vartheta] = \frac{\pi^2 m^2}{\beta E_c} + \frac{1}{4E_c} \int d\tau \dot{\vartheta}^2(\tau) + 2 \int d\tau \int d\tau' \alpha(\tau - \tau') \sin^2 \left[ \frac{\vartheta(\tau) - \vartheta(\tau')}{2} + \frac{\pi m(\tau - \tau')}{\beta} \right]. \quad (9)$$

From Eqs. (7) and (8), a convenient starting point for MC simulation is given by

$$\frac{E_c^*}{E_c} = \frac{2\pi^2}{\beta E_c} \frac{\sum_m m^2 \int D[\vartheta] \exp(-S_m[\vartheta])}{\sum_m \int D[\vartheta] \exp(-S_m[\vartheta])}. \quad (10)$$

which expresses  $E_c^*$  in terms of the mean squared winding number.

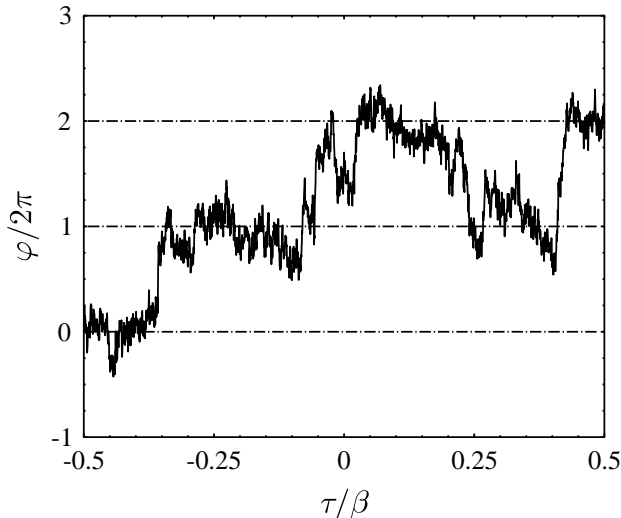


FIG. 2. Typical paths  $\varphi(\tau)$  generated in the MC simulation for large  $\alpha_t$  and low temperatures. Specifically, this configuration was present after 50,000 MC steps for  $\alpha_t = 30$  and  $\beta E_c = 500$ , taking  $\varphi(\tau) = 0$  initially.

For the MC simulation, we discretize imaginary time in  $P$  slices  $\tau_i$  of sufficiently small length  $\Delta\tau = \beta/P$ , and then sample  $\vartheta(\tau_i)$  and the winding number  $m$  from the action  $S_m[\vartheta]$  specified in Eq. (9). Measuring  $m^2$  along the MC trajectory allows to extract  $E_c^*$  according to Eq. (10). As is apparent from Eq. (8), the MC weight function is not necessarily positive definite for non-integer  $n_{\text{ex}}$ . The resulting interference can lead to numerical instabilities, especially near half-integer values of  $n_{\text{ex}}$ . The MC algorithm developed in Refs. [12,13] deals with the case of general  $n_{\text{ex}}$  and hence suffers from this problem. However, since we focus on the effective charging energy only and hence on the value  $n_{\text{ex}} = 0$ , there is no instability problem in our algorithm. This circumstance allowed us to reach temperatures of about one order of magnitude lower than studied in Ref. [12], typically  $\beta E_c = 500$ .

For a given parameter set  $(\alpha_t, \beta E_c)$ , we have first determined the Trotter number  $P$  by empirically checking convergence to the large- $P$  limit. Typically, a value of  $P = 5\beta E_c$  was sufficient. Special care is then necessary for large  $\alpha_t$  since the acceptance rates can be very low. The most important paths  $\varphi(\tau)$  encountered in this regime are of the form shown in Fig. 2. These paths closely resemble the multi-sluggon trajectories contributing to the semiclassical result (5) [14]. The predominant occurrence of these paths in the MC sampling gives a strong indication that the semiclassical sluggon calculus is indeed appropriate for large  $\alpha_t$ . The MC updating employs single-particle moves, where different samples are separated by five passes. Results reported below are obtained from several million samples per parameter set. The simulations were carried out on IBM RISC 6000/590

workstations.

Our data for the effective charging energy are shown in Fig. 3 together with the various analytical predictions [6,8–10,14] and the MC results by Falci *et al.* [12]. For weak tunneling, the zero-temperature limit was approached already for rather high temperatures,  $\beta E_c = 100$ . However, it turns out to be quite a demanding task to reach this limit for large  $\alpha_t$ . In fact, the data points for  $\alpha_t = 20$  and  $\alpha_t = 25$  (which were obtained for  $\beta E_c = 500$ ) are *not* in the true zero-temperature limit yet. This follows from comparing additional MC data obtained at different temperatures (not shown here) and has to be taken into account when comparing the finite-temperature MC data with the zero-temperature analytical predictions (4) and (5).

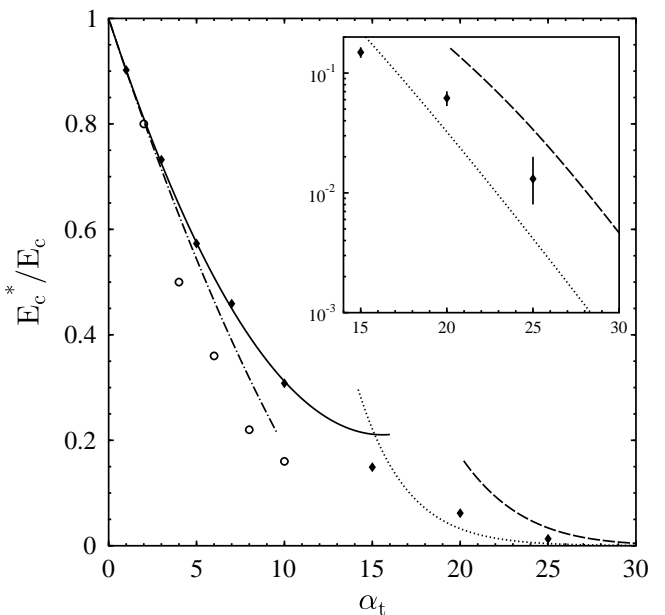


FIG. 3. MC data for  $E_c^*$  as a function of  $\alpha_t$  and comparison to previous work. The perturbative results for small  $\alpha_t$  are depicted as the dashed-dotted curve (see Golubev and Zaikin [9]) and the solid curve (see Grabert [8,10]), respectively. The analytical results for large  $\alpha_t$  are the dotted curve (for zero temperature, see Panyukov and Zaikin [6]) and the dashed curve (for  $\beta E_c = 500$ , see Wang and Grabert [14]), respectively. The MC data by Falci *et al.* [12] are shown as open circles, and our MC data are given by filled diamonds. In the inset, the data for large  $\alpha_t$  together with the curves from Refs. [6,14] are replotted on a semi-logarithmic scale. The data points were obtained at  $\beta E_c = 100$  for  $\alpha_t < 15$  and at  $\beta E_c = 500$  for  $\alpha_t \geq 15$ . Statistical errors on our MC data are smaller than the symbol size unless indicated by vertical bars.

For the case of *weak tunneling*, the theoretical predic-

tions by Grabert [8,10] given in Eq. (3) are confirmed with very good precision up to surprisingly large values of the tunneling conductance,  $\alpha_t \leq 10$ , while the NCA result (2) becomes inaccurate for  $\alpha_t > 5$ . We suspect that the discrepancy between the MC data of Ref. [12] and our results is due to the lower temperatures employed here. For  $\alpha_t \leq 15$ , our simulations have converged to the zero-temperature limit.

For the case of *strong tunneling*, the predictions of Panyukov and Zaikin [6] and of the sluggon calculus [14] differ by about one order of magnitude due to different pre-exponential factors, while our numerical data for  $\beta E_c = 500$  lie in between both predictions [19]. Since a further decrease of temperature will suppress thermal fluctuations even more, our MC results give a lower bound to the true zero-temperature result for  $E_c^*$ . However, the values of  $\alpha_t$  are still not large enough to confirm the sluggon prediction (5) unambiguously.

In conclusion, we have developed and carried out Monte Carlo simulations for the effective charging energy of the single electron box. The data describe a gradual smooth crossover between the analytically accessible limits of weak tunneling (where perturbation theory in the tunneling conductance applies) and strong tunneling (where a semiclassical calculus is appropriate).

The authors would like to thank G. Falci, G. Schön, and W. Zwerger for fruitful discussions. Financial support was provided by the Deutsche Forschungsgemeinschaft.

- [15] Lafarge, P., Pothier, H., Williams, E.R., Esteve, D., Urbina, C. and Devoret, M.H., *Z. Phys. B*, **85** (1991) 327; see also Esteve, D., in Ref. [1].
- [16] We note that the dimensionless conductance  $\alpha_t$  is related to the parameter  $g$  used in Refs. [5,8–10] by  $g = \alpha_t/4\pi^2$ .
- [17] The dimensionless conductance  $\alpha_t$  used by Panyukov and Zaikin (PZ) [6] is related to the tunneling conductance used here by  $\alpha_t^{\text{PZ}} = \alpha_t/4$ .
- [18] Ben-Jacob, E., Mottola, E. and Schön, G., *Phys. Rev. Lett.*, **51** (1983) 2064; Zaikin, A.D. and Schön, G., *Phys. Rep.*, **198** (1990) 237.
- [19] As the error bars on the MC data by Falci *et al.* [12] are very large for strong tunneling, we have only displayed their data for  $\alpha_t \leq 10$  in Fig. 3.

- 
- [1] *Single Charge Tunneling*, NATO ASI Series B294, ed. by Grabert, H. and Devoret, M.H. (Plenum, New York, 1992).
  - [2] Ingold, G.-L. and Nazarov, Yu.V., in Ref. [1].
  - [3] Zorin, A.B., Ahlers, F.-J., Niemeyer, J., Weimann, T. and Wolf, H., *Phys. Rev. B*, **53** (1996) 13 682.
  - [4] Guinea, F. and Schön, G., *Europhys. Lett.*, **1** (1986) 585.
  - [5] Matveev, K.A., *Zh. Eksp. Teor. Fiz.*, **99** (1991) 1598; (*Sov. Phys. JETP*, **72** (1991) 892).
  - [6] Panyukov, S.V. and Zaikin, A.D., *Phys. Rev. Lett.*, **67** (1991) 3168.
  - [7] Zwerger, W. and Scharpf, M., *Z. Phys. B*, **85** (1991) 421.
  - [8] Grabert, H., *Physica B*, **194-196** (1994) 1011.
  - [9] Golubev, D.S. and Zaikin, A.D., *Phys. Rev. B*, **50** (1994) 8736.
  - [10] Grabert, H., *Phys. Rev. B* **50** (1994) 17 364.
  - [11] Schoeller, H. and Schön, G., *Phys. Rev. B*, **50** (1994) 18 436.
  - [12] Falci, G., Schön, G. and Zimanyi, G.T., *Phys. Rev. Lett.*, **74** (1995) 3257.
  - [13] Heins, J., Diploma thesis, Universität Karlsruhe (1994).
  - [14] Wang, X. and Grabert, H., *Phys. Rev. B*, **53** (1996) 12 621.